Correlation and transport properties for mixtures at constant pressure and temperature

Alexander J. White,[1] Lee A. Collins,[1] Joel D. Kress,[1] Christopher Ticknor,[1] Jean Clérouin,[2] Philippe Arnault,[2] and Nicolas Desbiens[2]

[1]*Theoretical Division, Los Alamos National Laboratory, Los Alamos, New Mexico 87545, USA*

[2]*CEA, DAM, DIF, 91297 Arpajon, France*

(Received 10 March 2017; published 2 June 2017)

Transport properties of mixtures of elements in the dense plasma regime play an important role in natural astrophysical and experimental systems, e.g., inertial confinement fusion. We present a series of orbital-free molecular dynamics simulations on dense plasma mixtures with comparison to a global pseudo ion in jellium model. Hydrogen is mixed with elements of increasingly high atomic number (lithium, carbon, aluminum, copper, and silver) at a fixed temperature of 100 eV and constant pressure set by pure hydrogen at 2 g/cm^3, namely, 370 Mbars. We compute ionic transport coefficients, such as self-diffusion, mutual diffusion, and viscosity for various concentrations. Small concentrations of the heavy atoms significantly change the density of the plasma and decrease the transport coefficients. The structure of the mixture evidences a strong Coulomb coupling between heavy ions and the appearance of a broad correlation peak at short distances between hydrogen atoms. The concept of an effective one component plasma is used to quantify the overcorrelation of the light element induced by the admixture of a heavy element.

DOI: 10.1103/PhysRevE.95.063202

I. INTRODUCTION

Dense plasma mixtures are ubiquitous in the universe. Young stars as well as giant planets mix hydrogen with helium and traces of heavier elements, whereas white dwarf stars mix carbon with other high atomic number (Z) elements. Supernovas are subjected to violent shock waves creating heavy elements that blend with primordial hydrogen. Understanding of ionic transport in mixtures is required for the investigation of the composition of giant planets [1] and the sedimentation of heavy elements in white dwarf stars [2], for example. These systems fall in the regime of matter under extreme conditions and warm dense matter (WDM). Mixture properties also play a significant role in inertial confinement fusion. For example, mixing of the plastic ablator into the fuel has been used to partially explain lower than expected yields in experiments [3–6]. Understanding this behavior is crucial, so much so that experiments are designed to monitor and control mixing of the ablator into the fuel. Further motivation comes from the mixing of a gas-metal interface [7–9] that can trigger hydrodynamic instabilities [10]. In such cases, interfaces lead to strong concentration gradients and mixing.

The physics of these systems is driven by the ionization state corresponding to dense plasma. When there are many types of ions, then the ionization properties will vary between constituents, leading to very different Coulomb couplings between species. If direct simulation is a tool of choice to study mixtures, a global understanding of the mechanisms is still missing. Efforts to understand mixtures have typically taken on one of three approaches: mixing rules; simulations with model systems [such as the one component plasma (OCP) or Yukawa]; or direct simulations of mixtures. Mixing rules have proven successful for the equation of state by systematic comparisons with simulations [11–13]. They have also been shown to be reasonable for transport coefficients for LiH [12] and CH [14] mixtures, but less has been performed for more asymmetric mixtures. Models used to estimate transport properties include the OCP and its extension to binary ionic mixtures (BIMs) and Yukawa potentials. In the OCP and BIM models ions move in a uniform background of electrons. The Yukawa potential includes screening effects of the electrons. A shortcoming of these methods is that the ionizations and screening must be empirically determined. Typical approaches seek to produce an effective single component result for the transport properties, via the OCP and Yukawa models [15–19]. Large Yukawa molecular dynamics (MD) studies have explored the behavior of diffusion and viscosity for a fixed ion density, whereas the concentration is varied by simply swapping out ion types [20,21]. This paper found significant changes in both the diffusion and the viscosity as concentration was changed. Other recent work is based on quantum average atom models that account for correlations of ions via a hypernetted chain approximation [22,23] and then by using pseudoatom molecular dynamics [24], the entire equation of state can be obtained. The third approach is to perform direct simulations from first principles. This involves a variety of methods, all of which solve the electronic structure. For example quantum molecular dynamics using Kohn-Sham [25] or orbital-free MD (OFMD) [26] density functional theory, and path integral Monte Carlo [27,28]. Here we will focus on the use of OFMD, which has proven accurate for extracting equation-of-state and mass transport properties for the WDM regime and up to the hot dense plasmas regime [29–33].

We study a series of mixtures of hydrogen with increasing atomic number elements: lithium (H-Li), carbon (H-C), aluminum (H-Al), copper (H-Cu), and silver (H-Ag). To limit our study we have fixed the temperature at 100 eV and imposed isobaric conditions with reference to hydrogen at 2 g/cm^3. We systematically study how transport properties evolve with varying concentration for increasingly asymmetric mixtures. In the remaining paper we will first review OFMD methods and recall the pseudo ion in jellium (PIJ) model. Transport properties are compared with PIJ predictions. Structural properties are investigated through the various pair-distribution functions (PDFs).

II. METHODOLOGY

A. OFMD simulations of isobaric mixtures

We have performed large OFMD simulations of the various mixtures. We use the Born-Oppenheimer approximation and separate the electronic and ionic degrees of freedom, so for a given ion configuration, the electronic structure is computed at equilibrium. Then classical equations of motion for the ions are numerically integrated within the isokinetic ensemble [34]. The simulation has a total number N of ions in a volume V ($n = N/V$). N is the sum of all species $N = \sum_\gamma N_\gamma$ where, for the γth species, there are N_γ ions with nuclear charge Z_γ and atomic weight A_γ. Concentrations in number will be denoted by $\chi_Z = N_Z/N$ for the heavy element concentration. Additionally there are $N_e = \sum_\gamma N_\gamma Z_\gamma$ electrons in the volume.

The electronic density is found with a finite-temperature orbital-free density functional theory [26] treatment with the gradient correction form of Perrot [35] and the exchange correlation as a local density Perdew-Zunger form [36]. The electron-ion interaction is obtained from a regularization prescription [26] with a small enough cutoff radius to accommodate high pressures.

Extensive studies were taken to optimize both the time step and the fast Fourier transform (FFT) grid required to converge all properties. The FFT grids range between 128^3 and 256^3. A short time step of 0.6 a.u. is used to accurately resolve the hydrogen dynamics.

For the OFMD simulations, the total pressure of the system is

$$P = nk_BT + P_{\rm conf}(V,T). \tag{1}$$

This is the sum of the ideal gas pressure of the ions (at a constant T enforced by the isokinetic thermostat) and the configurational pressure $P_{\rm conf}$, computed via the forces on ions along trajectories and averaged after the system has equilibrated. In contrast with previous simulations on H-Ag [37] where we were interested in temperature scaling laws, the temperature is set here to 100 eV for all simulations. All mixtures are performed at the same pressure set by the pressure of pure hydrogen at 2 g/cm^3, 370 Mbars. The corresponding densities for pure Li, C, Al, Cu, and Ag at the same pressure, based on OFMD simulations, are 7.9, 9, 13.4, 21.6, and 30.9 g/cm^3, respectively. The density for an arbitrary mixture (Z,χ_Z) with $Z =$ Li, C, Al, Cu, or Ag, still at 370 Mbars due to pressure matching, is given by

$$\rho_{\rm mix} = \frac{(1-\chi_Z)A_1 + \chi_Z A_2}{(1-\chi_Z)V_1 + \chi_Z V_2}, \tag{2}$$

where (we denote by indices 1 and 2, the light and heavy species) $V_1 = A_1/\rho_1$ and $V_2 = A_2/\rho_2$ and ρ_1 and ρ_2 are the densities of pure elements corresponding to 370 Mbar.

We extract the transport properties from the mixture OFMD simulations [38,39]. The self-diffusion coefficient of a particular ion species D_γ is computed from the integral of the velocity autocorrelation function (VACF), which is as follows:

$$D_\gamma = \frac{1}{3}\int_0^\infty \langle \vec{v}_i(t)\cdot\vec{v}_i(0)\rangle dt, \tag{3}$$

where $\vec{v}_i$ is the velocity of the ith particle (γ species).

Mutual diffusion is found through the integral of a correlation function,

$$\begin{aligned} D_M &= \mathcal{J} D_{12} \\ &= \frac{\mathcal{J}}{3N\chi_1\chi_2}\int_0^\infty \langle A(t)A(0)\rangle dt, \\ A(t) &= \chi_2 \sum_i^{N_1} \vec{v}_i(t) - \chi_1 \sum_i^{N_2} \vec{v}_i(t), \end{aligned} \tag{4}$$

where $\mathcal{J}$ is a factor usually set to 1 [40] as we do here.

The shear viscosity was computed from the autocorrelation function of the stress tensor,

$$\eta = \frac{V}{k_BT}\int_0^\infty \langle P_{12}(t')P_{12}(0)\rangle dt' \tag{5}$$

for further details see Refs. [12,38].

We use empirical fits to the ACFs to shorten the duration of the trajectory required to converge the transport properties [31,41]. The statistical error inherent in computing correlation functions from molecular dynamics is estimated [42] as $\sqrt{2\tau/N_t dt}$ where $N_t dt$ is the length of the trajectory and τ is the correlation time of the ACF. We usually fit the ACF over a time interval of 0–4τ. The length of the simulation is much longer than τ. For the viscosity, the error computed is 10% or less for all simulations. The error for the self-diffusion is less than 5% due to the additional factor of $1/\sqrt{N_\gamma}$ from averaging the VACF over all of the ion types γ. The convergence was tested for high temperature simulations with H.

The correlation time scales of the viscosity and the mutual diffusion are typically long compared to self-diffusion time scales. To converge all properties required a large number of time steps.

Densities of the various mixtures versus concentration in the heavy elements are reported in Fig. 1(a) and in Table I. We emphasize the fact that all points representative of a thermodynamic state (Z,χ_Z) are at the same pressure of 370 Mbars. The symbols represent densities actually used in the simulations, and the lines represent the prediction of the simple isobaric model used in the PIJ model (see below).

B. PIJ model for isobaric mixtures

In the PIJ model, the viscosity and the diffusion coefficients are computed from the input of the temperature, density, and composition of the mixture. For the isobaric mixtures, the pressure is given, and the density varies with the composition (see Fig. 1), namely, with the heavy element concentration χ_Z. Therefore, we added a simple isobaric model of the equation of state in order to provide PIJ model predictions at any value of χ_Z. In this high density high temperature regime, the pressure can be estimated precisely by a OCP contribution [43] for the ions $P_{\rm OCP}$ and an electronic contribution $P_{\rm ele}$ [44] deduced from the Thomas-Fermi (TF) ionization $Q_{\rm TF}$ [45],

$$\frac{P_{\rm OCP}}{nk_BT} = 1 + \frac{1}{3}[0.94544\Gamma^{1/4} + 0.17954\Gamma^{-1/4} - 0.80049], \tag{6a}$$

$$P_{\rm ele}/n_e = \left[(k_BT)^3 + 3.36n_e(k_BT)^{3/2} + \frac{9\pi^4}{125}n_e^2\right]^{1/3}, \tag{6b}$$

TABLE I. OFMD simulations. Density, self-diffusion of hydrogen and heavy elements, mutual diffusion, and viscosity for H-Li, H-C, H-Al, H-Cu, and H-Ag mixtures at 100 eV and 370 Mbars. Density is expressed in g/cm^3, diffusion is expressed in cm^2/s, and viscosities are expressed in Pa s.

	OFMD results																											
	H-Li					H-C					H-Al					H-Cu					H-Ag							
χ_Z	ρ	D_H	D_{Li}	D_{12}	η	ρ	D_H	D_C	D_{12}	η	ρ	D_H	D_{Al}	D_{12}	η	ρ	D_H	D_{Cu}	D_{12}	η	ρ	D_H	D_{Ag}	D_{12}	η			
0.00	2	1.52			0.183	2	1.52			0.183	2	1.52			0.183	2	1.52			0.183	2	1.52			0.183			
0.05	2.5	1.29	0.26	0.30	0.170	2.86	1.12	0.111	0.15	0.136	3.98	0.92	0.048	0.106	0.106	6.57	0.78	0.021	0.066	0.074	9.73	0.68	0.0133	0.055	0.065			
0.10	2.97	1.18	0.23	0.34	0.132	3.59	0.93	0.089	0.15	0.097	5.50	0.66	0.034	0.112	0.062	9.67	0.57	0.015	0.078	0.054	14.6	0.51	0.0085	0.062	0.042			
0.25	4.18	0.92	0.16	0.36	0.124	5.28	0.69	0.060	0.21	0.056	8.51	0.51	0.022	0.161	0.033	14.9	0.41	0.0096	0.106	0.026	22.4	0.36	0.0066	0.086	0.027			
0.50	5.76	0.77	0.12	0.42	0.074	7.09	0.53	0.045	0.30	0.036	11.1	0.43	0.018	0.210	0.020	18.7	0.37	0.0086	0.192	0.021	27.6	0.31	0.0056	0.152	0.021			
0.75	6.96	0.71	0.10	0.57	0.060	8.23	0.47	0.041	0.38	0.025	12.5	0.38	0.016	0.310	0.017	20.5	0.34	0.0082	0.244	0.016	29.0	0.31	0.0055	0.236	0.020			
1.00	7.90		0.09		0.042	9.02		0.037		0.018	13.4		0.015		0.013	21.6		0.0079		0.016	30.9		0.0051		0.019			

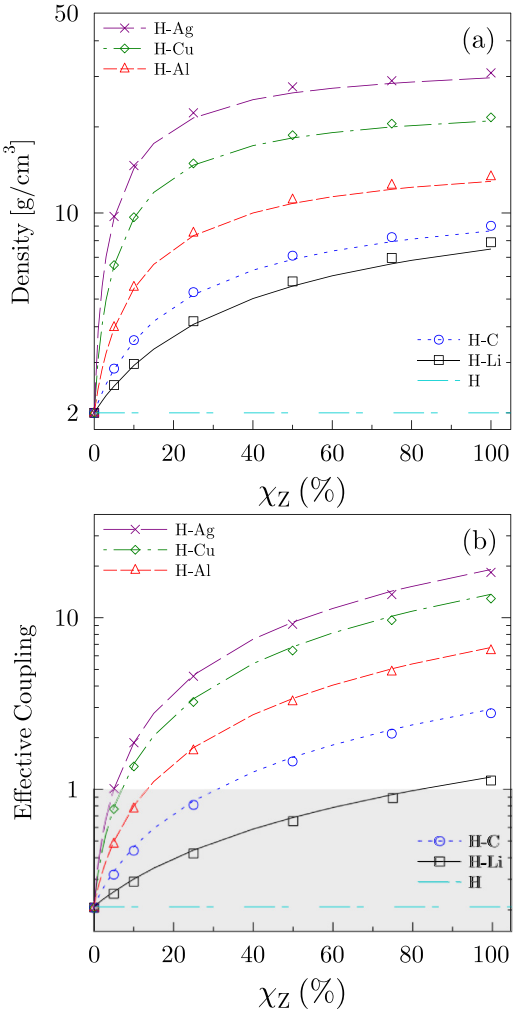

FIG. 1. (a) Densities of mixtures versus χ_Z. The symbols represent densities actually used in the OFMD simulation and the resulting effective coupling parameter $\Gamma_{\rm eff}$. The lines represent the prediction of the simple isobaric model used in the PIJ model. (b) $\Gamma_{\rm eff}$ versus heavy element concentration χ_Z for H-Li [(black squares) (solid line)], H-C [(blue circles) (dotted line)], H-Al [(red triangles) (dashed line)], H-Cu [(green triangles) (dashed-dot line)], H-Ag [(violet crosses) (long dashed line)], and pure H (teal long dashed and short dashed lines). The gray area defines the weak coupling region where kinetic formulation is the main contribution $\Gamma_{\rm eff} < 1$.

where $n_e = Q_{\rm TF} n$ and atomic units are used for this latter (1 a.u. of pressure = 294 Mbars). The Coulomb coupling parameter Γ is defined by

$$\Gamma = \frac{Q^2 e^2}{a k_B T}, \tag{7}$$

where a is the mean ion sphere radius $a = (3/4\pi n)^{1/3}$. With this simple model, the hydrogen pressure at 2 g/cm^3 and 100 eV is 378 Mbars instead of the targeted pressure of the OFMD equal to 370 Mbars. The corresponding densities for pure Li, C, Al, Cu, and Ag at the same pressure are 7.5, 8.7, 12.9, 21, and 29.7 g/cm^3, respectively, instead of 7.9, 9, 13.4, 21.6, and 30.9 g/cm^3 in the OFMD simulations. Using Eq. (2), we obtained the corresponding densities for mixtures in this

simple model, plotted in Fig. 1(a). They are about 3% less than the OFMD densities.

For pure elements, the PIJ model relies on the OCP with the Thomas-Fermi ionization $Q_{\rm TF}$. For binary mixtures, it relies on the BIM with a prescription giving the ionizations Q_1 and Q_2 and the average volumes by atom of each species V_1 and V_2. Requiring electroneutrality, additivity of volumes and a constant electron density, leads to

$$\frac{V_1}{Q_1} = \frac{V_2}{Q_2}, \tag{8a}$$

$$N_1 V_1 + N_2 V_2 = V. \tag{8b}$$

This system of equations is closed with the calculation of the ionization Q_γ as a function of T and V_γ in the Thomas-Fermi approximation. Once the ionization Q_γ and the partial volume V_γ are known, it is possible to compute a coupling parameter $\Gamma_\gamma = Q_\gamma^2 e^2/a_\gamma k_B T$, $a_\gamma = (3V_\gamma/4\pi)^{1/3}$ for each component and an effective coupling parameter $\Gamma_{\rm eff} = \chi_1\Gamma_1 + \chi_2\Gamma_2$ for the mixture.

For the asymmetric mixtures considered here at $T =$ 100 eV, the light element (hydrogen) is weakly coupled with $\Gamma \sim 0.2$. On the contrary, the heavy element is more coupled, $\Gamma \sim 1$ for lithium and $\Gamma \sim 20$ for silver. Figure 1(b) shows that the effective coupling $\Gamma_{\rm eff}$ smoothly interpolates across coupling regimes calling for a theory able to treat both limits. In particular, one can see that the H-Li mixture always stays moderately coupled ($\Gamma_{\rm eff} < 1$), whereas the H-Ag mixture reaches a strongly coupled regime as soon as the heavy element concentration is higher than 10%.

The global PIJ model for self- and mutual diffusion and for viscosity is presented in Refs. [18,37]. The main idea is to gather, in a single scheme, kinetic and coupled evaluations of transport coefficients reflecting the thermodynamic state of the mixture (Z, χ_Z) shown in Fig. 1(b). In the kinetic regime, we choose the straightforward Fokker-Planck-Landau (FPL) formulation in terms of collision frequencies which reduces to Chapman-Enskog (CE) at first order. The CE second order brings in the relaxation corrections naturally. Moreover, the effective potential theory of Stanton and Murillo [19] and Daligault *et al.* [46] extends this solution into the coupled regime up to $\Gamma \simeq 10$.

1. Kinetic regime

In the kinetic regime, transport coefficients are given using collision frequency estimates,

$$\eta^{\rm FPL} = K_1 \frac{n_1 k_B T}{\tilde{\nu_1}} + K_2 \frac{n_2 k_B T}{\tilde{\nu_2}}, \tag{9a}$$

$$D_{12}^{\rm FPL} = R_{12} c_2 \frac{k_B T}{\nu_{12}} \frac{\bar{m}}{m_1 m_2}, \tag{9b}$$

$$D_\alpha^{\rm FPL} = R_\alpha \frac{1}{\tilde{\nu_\alpha}} \frac{k_B T}{m_\alpha}, \quad \alpha = 1,2, \tag{9c}$$

where m_α is the mass of component α, c_α is its mass concentration, $n_\alpha = N_\alpha/V$, and $\bar{m} = \chi_1 m_1 + \chi_2 m_2$. The collision frequencies are defined for Maxwellian distributions by

$$\nu_{\alpha\beta} = \frac{n_\beta}{m_\alpha} \frac{4\sqrt{2\pi m_{\alpha\beta}} Q_\alpha^2 Q_\beta^2 e^4 \ln \Lambda_{\alpha\beta}}{3(k_B T)^{3/2}}, \tag{10}$$

where $\ln \Lambda_{\alpha\beta}$ is the Coulomb logarithm for $\alpha\beta$ interactions and $m_{\alpha\beta} = m_\alpha m_\beta/(m_\alpha + m_\beta)$ is the reduced mass. The total collision frequencies for each species are $\tilde{\nu_1} = \nu_{11} + \nu_{12}$ and $\tilde{\nu_2} = \nu_{22} + \nu_{21}$. When hydrogen is mixed with a highly ionized heavy element of charge Q_Z, the collisions involving Q_Z become quickly dominant: $\tilde{\nu_1} \sim \nu_{12}$ and $\tilde{\nu_2} \sim \nu_{22}$ with a strength proportional to Q_Z^2 and Q_Z^4, respectively. This situation is characteristic of the transition to a Lorentz gas behavior [37]. K_1, K_2, R_1, R_2, and R_{12} are correction factors with respect to the Maxwellian estimate of the collision frequencies. These factors are called relaxation corrections since they have been evaluated by solving the linearized kinetic equations to obtain the corrections to the Maxwellian distributions associated with small gradients of density, velocity, and temperature. Baalrud and Daligault [47] and Shaffer *et al.* [48] found that the relaxation corrections tend to 1 at high coupling. In the moderate to strong coupling regime of the present cases, we indeed found the best agreement with OFMD results using $R_1 = R_2 = R_{12} = 1.19$, the pure element value [49]. Viscosity is less sensitive to this issue, and we kept $K_1 = 0.965$ and K_2 as given in our previous paper [37].

In the PIJ model, the transition from the weakly coupled regime to the strongly coupled regime is realized by the introduction of contributions in excess of the kinetic results,

$$\eta = \eta^{\rm FPL} + \eta_{\rm ex}, \tag{11a}$$

$$D = D^{\rm FPL} + D_{\rm ex}. \tag{11b}$$

This requires a bounded Coulomb logarithm in order to avoid divergencies at high coupling,

$$\ln \Lambda \longrightarrow \max(\ln \Lambda, L_0) \quad \text{with } L_0 = 1.65. \tag{11c}$$

A smooth transition across coupling regimes is then achieved at $\Gamma_{\rm eff} \sim 0.15$.

2. Coupled regime

In the coupled regime, we use mixing rules to estimate the excess contributions $D_{\rm ex}$ and $\eta_{\rm ex}$. For the viscosity, we define an equivalent OCP of charge $Q_{\rm eff}$, corresponding to the effective coupling $\Gamma_{\rm eff}$ of the mixture, and evaluate $\eta_{\rm ex}$ as

$$\eta_{\rm ex} = \eta_{\rm OCP}(Q_{\rm eff}, V, T) - \eta^{\rm FPL}(Q_{\rm eff}, V, T). \tag{12a}$$

For the self-diffusion, we define $D_{\alpha,\rm ex}$ as

$$D_{\alpha,\rm ex} = D_{\rm OCP}(Q_\alpha, V_\alpha, T) - D^{\rm FPL}(Q_\alpha, V_\alpha, T). \tag{12b}$$

For the mutual diffusion, we apply the Darken relation to the excess self-diffusions,

$$D_{12,\rm ex} = \chi_1 D_{2,\rm ex} + \chi_2 D_{1,\rm ex}. \tag{12c}$$

The OCP diffusion and viscosity are obtained from published fits [16,50]. The results for densities and transport properties in the PIJ model are gathered in Table II.

TABLE II. The PIJ model. Density, self-diffusion of hydrogen and heavy elements, mutual diffusion, and viscosity for H-Li, H-C, H-Al, H-Cu, and H-Ag mixtures at 100 eV at a pressure of 378 Mbars. The units are same as in Table I.

	PIJ model results																							
	H-Li					H-C					H-Al					H-Cu					H-Ag				
χ_Z	ρ	D_H	D_{Li}	D_{12}	η	ρ	D_H	D_C	D_{12}	η	ρ	D_H	D_{Al}	D_{12}	η	ρ	D_H	D_{Cu}	D_{12}	η	ρ	D_H	D_{Ag}	D_{12}	η
0.00	2	1.59			0.204	2.	1.59			0.204	2.	1.59			0.204	2	1.59			0.204	2	1.59			0.204
0.05	2.548	1.34	0.19	0.28	0.170	2.84	1.02	0.057	0.12	0.126	3.95	0.70	0.021	0.059	0.082	6.56	0.52	0.010	0.037	0.061	9.61	0.46	0.0071	0.030	0.056
0.10	2.93	1.18	0.16	0.29	0.147	3.56	0.81	0.049	0.13	0.092	5.44	0.56	0.020	0.075	0.060	9.60	0.43	0.0097	0.052	0.046	14.3	0.39	0.0066	0.045	0.041
0.25	4.08	0.93	0.13	0.35	0.100	5.18	0.60	0.041	0.19	0.057	8.33	0.44	0.018	0.13	0.036	14.7	0.37	0.0089	0.099	0.028	21.5	0.35	0.0060	0.091	0.027
0.50	5.55	0.75	0.11	0.44	0.067	6.88	0.51	0.037	0.27	0.035	10.8	0.40	0.017	0.21	0.023	18.3	0.34	0.0084	0.176	0.020	26.3	0.33	0.0057	0.167	0.021
0.75	6.64	0.67	0.10	0.53	0.048	7.94	0.47	0.036	0.36	0.025	12.1	0.38	0.016	0.29	0.018	20.0	0.33	0.0082	0.253	0.017	28.4	0.32	0.0056	0.242	0.019
1.00	7.48		0.09		0.035	8.66		0.034		0.019	12.9		0.016		0.015	21.0		0.0081		0.016	29.7		0.0055		0.020

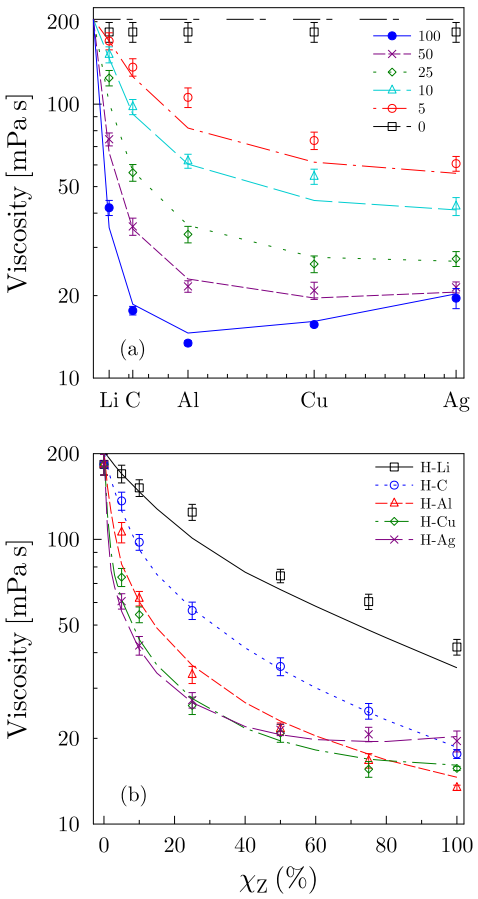

FIG. 2. (a) Viscosity η (mPa s) of the H-Z mixture as a function of the atomic number of the high mass component (symbols: OFMD simulations; lines: the PIJ model), $\chi_Z = 0.00$ (squares, long dashed, and short dashed lines), 0.05 (circle, long dashed-dotted line), 0.10 (triangles, long dashed line), 0.25 (diamond, dotted line), 0.50 (cross, dashed line), and 1.00 (filled circles, solid line). (b) (Alternate view) Viscosity as a function of χ_Z for H-Z mixtures (symbols: OFMD simulations; lines: the PIJ model, see Fig. 1). All simulations are at a temperature of $kT = 100$ eV and pressure matched to 100% H at 2.00 g/cm^3.

III. TRANSPORT PROPERTIES

A. Viscosity

The viscosity is the product of two contributions, kinetic and potential, to the stress tensor. The kinetic part is the main contribution for hydrogen, whereas the potential part becomes increasingly important with high-Z elements. This behavior is illustrated in Fig. 2(a) for pure materials [(blue filled circles) (solid line)] where the viscosity as a function of Z at first drops due to the weakening of the kinetic contribution and then increases for high-Z materials as the potential contribution becomes dominant. The minimum occurs near aluminum and is captured by the PIJ model (lines), which shows good agreement for all data.

Figure 2(b) shows, in an alternative representation, the behavior of the viscosity for a given mixture when the concentration χ_Z of the heavy element is varied. As a heavy element is added to hydrogen, the viscosity first decreases, and in high-Z cases, it stabilizes or even increases at high

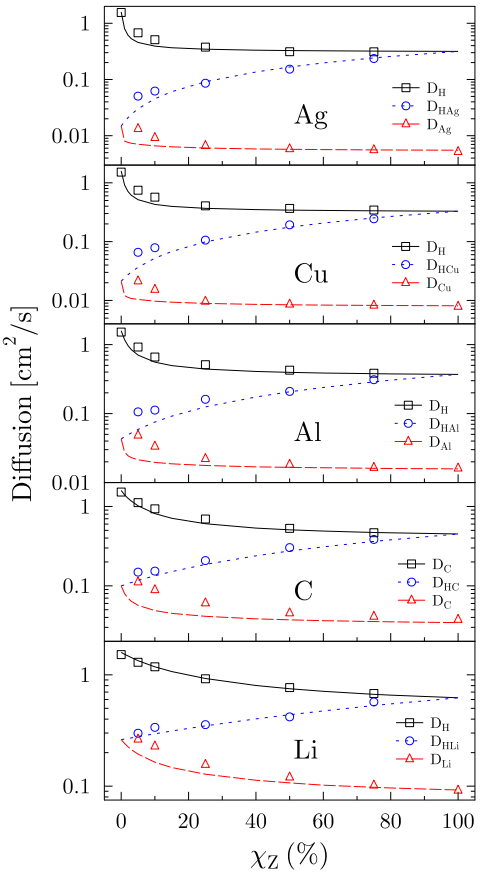

FIG. 3. Self-diffusion for hydrogen D_H [(black circles) (solid line)], high-Z self-diffusion D_Z [(red triangles) (dashed line)], and mutual-diffusion $D_{H\text{-}Z}$ [(blue circle) (dotted line)] as a function of χ_Z. From top to bottom: H-Ag, H-Cu, H-Al, H-C, and H-Li mixtures (symbols: OFMD simulations; lines: the PIJ model).

concentrations. The rapid rise of the effective coupling Γ_{eff}, shown in Fig. 1(b), drives the system from the region where the kinetic contribution dominates the stress tensor to the region where the main contribution comes from the potential part. The first weakening of the viscosity is stronger for higher atomic numbers. For a nearly symmetric mixture, such as H-Li, this effect is almost linear reflecting the slow increase in Γ_{eff} in this case [see Fig. 1(b)]. For all mixtures, the PIJ model yields accurate results for the viscosity, only beginning to deviate at small concentrations of the heavy component. For the H-Li mixture, the PIJ slightly underestimates the viscosity for all concentrations.

B. Diffusion

In Fig. 3 the overall behavior of diffusion coefficients is gathered for all mixtures considered. OFMD simulations are represented by symbols, and the PIJ model is represented by the corresponding lines. Corresponding data are given in Tables I and II. The hydrogen self-diffusion is strongly influenced by the proportion in heavy elements: It is strongly lowered with the addition of a 10% heavy element and is less varied for higher concentrations. The heavy component self-diffusion is not as strongly influenced by hydrogen

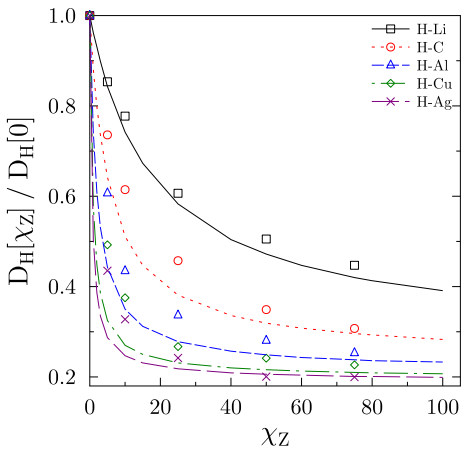

FIG. 4. Hydrogen self-diffusion D_H for varied concentration, normalized by pure hydrogen diffusion [OFMD: symbols, PIJ: solid line, see Fig. 2(b)].

concentration, except at low concentrations (high hydrogen concentration) where the heavy element self-diffusion is enhanced. The mutual diffusion follows the behavior predicted by the Darken relation, interpolating between the self-diffusion of the heavy element at low heavy element concentration and of hydrogen self-diffusion at high heavy element concentration. The Darken relation is an excellent approximation to the mutual diffusion with deviations typically within the 10% statistical error of the OFMD results. The PIJ model reproduces the global trends of these transport coefficients but underestimates the enhancement of high-Z self-diffusion at low concentrations, predicting only a sharp enhancement very close to $\chi_Z = 0$.

In Fig. 4 we plot the diffusion of hydrogen in the mixtures relative to the pure hydrogen diffusion. Weakly interacting hydrogen atoms will exhibit a high diffusion coefficient due to the long mean-free path of the particles. The introduction of high-Z particles into the system will provide scattering centers which rapidly reduce this mean-free path, leading to Lorentz-type diffusion. Higher-Z components result in two effects: (1) a stronger suppression of D_H in the $\chi_Z = 1$ limit (Fig. 4) and (2) a more rapid decrease at small χ_Z and a saturation of the D_H, reaching almost a plateau, at higher χ_Z. The PIJ model reproduces the reduction of the light element self-diffusion under mixing with a heavy element within 10%–30% accuracy.

IV. STRUCTURE OF MIXTURES

A structural description of the mixtures is given by the radial PDFs,

$$g_{\lambda,\gamma}(r) = \frac{V}{N_\lambda N_\gamma}\left\langle \sum_i^{N_\lambda} \sum_{j\neq i}^{N_\gamma} \delta(r - r_{ij}) \right\rangle, \tag{13}$$

which is the ratio of the number density of species γ to the ideal gas number density at a distance r away from a particle of species λ.

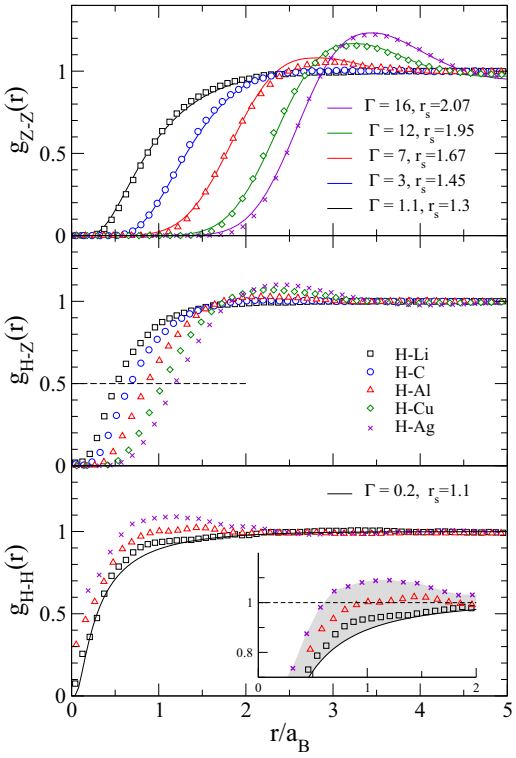

FIG. 5. Radial pair distribution functions for different mixtures at 75% heavy element (Z), 25% hydrogen: Top: Z-Z, middle: H-Z, bottom: H-H. The bottom inset, a closer view of the H-H correlation feature [OFMD: symbols, see Fig. 2(b); EOCP: solid lines]. We emphasize that the lines are the EOCP model not the lines drawn between symbols. The gray area in the inset corresponds to the region of overcorrelation between hydrogens compared to their pure element values (the black solid line at $\Gamma = 0.2$).

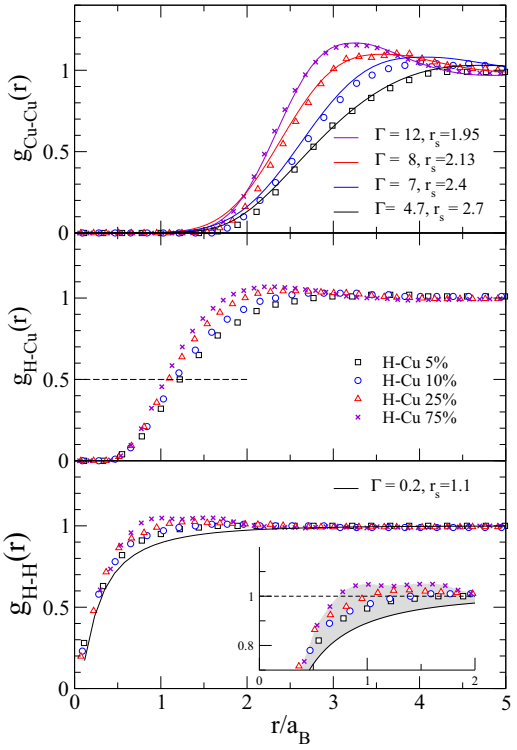

FIG. 6. Radial pair-distribution functions for different concentrations of Cu in the H-Cu mixture: top: Cu-Cu; middle: H-Cu; bottom: H-H. The bottom inset, closer view of the H-H correlation feature. Squares: 5% Cu; circles: 10% Cu; triangles: 25% Cu; cross: 75% Cu. The full lines are the EOCP model, and the gray area in the inset is the overcorrelation region.

A. The effective one component plasma concept

The correlations between species can be unambiguously characterized by the effective one component plasma (EOCP) concept [51]. It consists of searching for the best agreement of the actual PDF with the one generated by the OCP model at a given coupling parameter Γ. A first application was the evidence of persistence of correlations for a system subjected to isochoric heating: the Γ plateau [52,53]. Efficient fits of the OCP's structural properties are now available in a wide range of couplings [54]. OCP PDFs being expressed in reduced units of distance ($r^* = r/a$ with a being the ion-sphere radius), the passage to atomic units needs to multiply distances by $r_s = a/a_B$ (where a_B is the Bohr radius). This is why r_s is mentioned in Figs. 5 and 6. The relation between r_s and ρ is given by $\rho = 2.678\,847(A/r_s^3)$ g/cm^3 with A as the atomic mass.

B. Varying the heavy element

In Fig. 5, the PDFs of the 25% hydrogen 75% high-Z mixtures are plotted. The high-Z-high-Z PDFs (top panel) show a standard progression from moderately correlated Li and C to strongly correlated Cu and Ag. These structures are well reproduced by the corresponding EOCP with coupling parameters ranging from 16 for Ag-Ag correlations to 1.1 for Li-Li correlations (continuous lines in the top panel).

The H-high-Z PDFs (middle panel) are beyond an EOCP description. This cross correlation shows that the void due to interparticle repulsion strongly depends on the atomic number Z. Indeed, the radius for which the PDF reaches the value of 1/2 (horizontal dashed line in Fig. 5) is a measure of the coupling intensity [55]. In addition, for high-Z elements we observe the emergence of a correlation peak between the hydrogen and the heavy atom.

The H-H PDFs (bottom panel) in the presence of heavier elements show some overcorrelation when compared to the EOCP for pure hydrogen at 2 g/cm^3 and 100 eV ($\Gamma = 0.2$, $r_s = 1.1$). The EOCP perfectly fits a pure hydrogen simulation. This overcorrelation is visible even with the less asymmetric mixture (hydrogen with lithium) when compared to the pure hydrogen situation. This effect is different in its nature from Coulombic correlations in plasmas of pure elements. It leads to a broad peak in the PDF and a reduction of the H-H interatomic void, i.e., the hydrogens are forced closer together. This correlation is qualitatively different from the correlation that is present in an EOCP model.

Such clustering of low-Z atoms in very asymmetric binary ionic mixtures has been observed previously by Whitley *et al.* [56] with large scale classical molecular dynamics simulations.

C. Varying the concentration of the heavy element

In Fig. 6 we plot the PDFs of the H-Cu mixtures for different concentrations of Cu. Lowering the concentration of Cu leads to a loss of the Cu-Cu correlation, starting from $\Gamma = 12$ at 75% concentration to $\Gamma = 4.7$ at 5% according to the EOCP. Interestingly, the correlations between hydrogen and copper are weakly affected by copper concentration over the wide range of concentrations [horizontal dashed line in Fig. 6 (middle)].

A comparison with the EOCP for pure hydrogen [Fig. 6 (bottom)] shows that, even for the smallest concentration of Cu (5%), the H-H PDF is still more structured than the pure hydrogen represented by the solid line. The overcorrelation effect discussed above appears as soon as the heavy element is introduced in hydrogen, even in small proportions.

V. CONCLUSION

We have performed simulations of binary mixtures of hydrogen and higher atomic number elements (Li, C, Al, Cu, and Ag) in variable proportions (from 0% to 100%) in the warm dense plasma regime. Our simulations are at P-T equilibrium (100 eV and 370 Mbars) thus density changes for the different mixtures. Behavior across different Z's and concentrations of high-Z elements were discussed.

Dramatic changes in the viscosity and self-diffusion are seen in the area of low concentration of high-Z elements. The steepness of these changes increases with Z. A transition from kinetic to coupled regimes is visible in the viscosities and high-Z self-diffusion of the mixtures. We compare orbital-free molecular dynamics with a global pseudo ion in jellium model (no molecular dynamics required). The PIJ model reproduces the qualitative features of the χ_Z and Z dependences and nearly quantitatively reproduces viscosities for these mixtures. At low χ_Z the PIJ underestimates both self-diffusions. We intend to improve the kinetic part of the PIJ model following the work of Baalrud and Daligault [47].

We have investigated the structure of the mixtures by analyzing the pair-distribution functions. With an admixture of heavy elements, a broad correlation peak appears at short distances between H atoms. Using an effective one component plasma model to gauge the intensity of the correlations, we have quantified this effect. Even for the smallest-Z element, lithium or for copper at the smallest concentration (5%), this overcorrelation effect is noticeable. It is our intention to show in a future paper how these overcorrelation effects of hydrogen in the presence of heavy elements translates into an enhancement of nuclear reactions [56].

ACKNOWLEDGMENTS

The authors gratefully acknowledge support from Advanced Simulation and Computing, Science Campaigns 1 and 4, computing resource from ATCC and LANL, which is operated by LANS, LLC for the NNSA of the U.S. DOE under Contract No. DE-AC52-06NA25396. This work has been performed under the NNSA/DAM collaborative Agreement No. P184 on Basic Science. We especially thank F. Lambert for providing his OFMD code.

[1] D. Bruno, C. Catalfamo, M. Capitelli, G. Colonna, O. De Pascale, P. Diomede, C. Gorse, A. Laricchiuta, S. Longo *et al.*, Phys. Plasmas **17**, 112315 (2010).
[2] J. Hughto, A. S. Schneider, C. J. Horowitz, and D. K. Berry, Phys. Rev. E **82**, 066401 (2010).
[3] V. A. Smalyuk, L. J. Atherton, L. R. Benedetti, R. Bionta, D. Bleuel, E. Bond, D. K. Bradley, J. Caggiano, D. A. Callahan *et al.*, Phys. Rev. Lett. **111**, 215001 (2013).
[4] M. J. Edwards, P. K. Patel, J. D. Lindl, L. J. Atherton, S. H. Glenzer, S. W. Haan, J. D. Kilkenny, O. L. Landen, E. I. Moses, A. Nikroo *et al.*, Phys. Plasmas **20**, 070501 (2013).
[5] H. F. Robey, B. J. MacGowan, O. L. Landen, K. N. LaFortune, C. Widmayer, P. M. Celliers, J. D. Moody, J. S. Ross, J. Ralph, S. LePape *et al.*, Phys. Plasmas **20**, 052707 (2013).
[6] H. G. Rinderknecht, H. Sio, C. K. Li, A. B. Zylstra, M. J. Rosenberg, P. Amendt, J. Delettrez, C. Bellei, J. A. Frenje, M. Gatu Johnson *et al.*, Phys. Rev. Lett. **112**, 135001 (2014).
[7] K. Molvig, E. L. Vold, E. S. Dodd, and S. C. Wilks, Phys. Rev. Lett. **113**, 145001 (2014).
[8] K. Molvig, A. N. Simakov, and E. L. Vold, Phys. Plasmas **21**, 092709 (2014).
[9] L. Welser-Sherrill, J. Fincke, F. Doss, E. Loomis, K. Flippo, D. Offermann, P. Keiter, B. Haines, and F. Grinstein, High Energy Density Phys. **9**, 496 (2013).
[10] M. Vandenboomgaerde, M. Bonnefille, and P. Gauthier, Phys. Plasmas **23**, 052704 (2016).
[11] F. Lambert, J. Clérouin, J.-F. Danel, L. Kazandjian, and G. Zérah, Phys. Rev. E **77**, 026402 (2008).
[12] L. Burakovsky, C. Ticknor, J. D. Kress, L. A. Collins, and F. Lambert, Phys. Rev. E **87**, 023104 (2013).
[13] J.-F. Danel and L. Kazandjian, Phys. Rev. E **91**, 013103 (2015).
[14] F. Lambert and V. Recoules, Phys. Rev. E **86**, 026405 (2012).
[15] J. G. Clérouin, M. H. Cherfi, and G. Zérah, Europhys. Lett. **42**, 37 (1998).
[16] S. Bastea, Phys. Rev. E **71**, 056405 (2005).
[17] S. Bastea, Phys. Rev. E **75**, 031201 (2007).
[18] P. Arnault, High Energy Density Phys. **9**, 711 (2013).
[19] L. G. Stanton and M. S. Murillo, Phys. Rev. E **93**, 043203 (2016).
[20] T. Haxhimali, R. E. Rudd, W. H. Cabot, and F. R. Graziani, Phys. Rev. E **90**, 023104 (2014).
[21] T. Haxhimali, R. E. Rudd, W. H. Cabot, and F. R. Graziani, Phys. Rev. E **92**, 053110 (2015).
[22] C. E. Starrett and D. Saumon, Phys. Rev. E **85**, 026403 (2012).
[23] C. E. Starrett, D. Saumon, J. Daligault, and S. Hamel, Phys. Rev. E **90**, 033110 (2014).
[24] C. E. Starrett, J. Daligault, and D. Saumon, Phys. Rev. E **91**, 013104 (2015).
[25] A. Pribram-Jones, S. Pittalis, E. Gross, and K. Burke, in *Frontiers and Challenges in Warm Dense Matter*, edited by F. Graziani, M. P. Desjarlais, R. Redmer, and S. B. Trickey, Lecture Notes in Computational Science and Engineering Vol. 96 (Springer, Berlin, 2014), pp. 25–60.

[26] F. Lambert, J. Clérouin, and G. Zérah, Phys. Rev. E **73**, 016403 (2006).
[27] S. A. Bonev, B. Militzer, and G. Galli, Phys. Rev. B **69**, 014101 (2004).
[28] B. Militzer and K. P. Driver, Phys. Rev. Lett. **115**, 176403 (2015).
[29] J. D. Kress, J. S. Cohen, D. A. Horner, F. Lambert, and L. A. Collins, Phys. Rev. E **82**, 036404 (2010).
[30] J. D. Kress, J. S. Cohen, D. P. Kilcrease, D. A. Horner, and L. A. Collins, Phys. Rev. E **83**, 026404 (2011).
[31] D. A. Horner, J. D. Kress, and L. A. Collins, Phys. Rev. B **77**, 064102 (2008).
[32] D. A. Horner, F. Lambert, J. D. Kress, and L. A. Collins, Phys. Rev. B **80**, 024305 (2009).
[33] C. Ticknor, L. A. Collins, and J. D. Kress, Phys. Rev. E **92**, 023101 (2015).
[34] P. Minary, G. J. Martyna, and M. E. Tuckerman, J. Chem. Phys. **118**, 2510 (2003).
[35] F. Perrot, Phys. Rev. A **20**, 586 (1979).
[36] J. P. Perdew and A. Zunger, Phys. Rev. B **23**, 5048 (1981).
[37] C. Ticknor, J. D. Kress, L. A. Collins, J. Clérouin, P. Arnault, and A. Decoster, Phys. Rev. E **93**, 063208 (2016).
[38] M. P. Allen and D. J. Tildesley, *Computer Simulations of Liquids* (Oxford University Press, Oxford, 2009).
[39] D. Alfè and M. J. Gillan, Phys. Rev. Lett. **81**, 5161 (1998).
[40] J. P. Hansen and I. R. McDonald, *Theory of Simple Liquids*, 3rd ed. (Elsevier, London/Burlington, MA, 2006).
[41] E. R. Meyer, J. D. Kress, L. A. Collins, and C. Ticknor, Phys. Rev. E **90**, 043101 (2014).
[42] R. Zwanzig and N. K. Ailawadi, Phys. Rev. **182**, 280 (1969).
[43] W. L. Slattery, G. D. Doolen, and H. E. DeWitt, Phys. Rev. A **21**, 2087 (1980).
[44] A. F. Nikiforov, V. G. Novikov, and V. B. Urarov, *Quantum-Statistical Models of Hot Dense Matter* (Springer, Berlin, 2005).
[45] D. Salzmann, *Atomic Physics in Hot Plasmas* (Oxford University Press, Oxford, 1998).
[46] J. Daligault, S. D. Baalrud, C. E. Starrett, D. Saumon, and T. Sjostrom, Phys. Rev. Lett. **116**, 075002 (2016).
[47] S. D. Baalrud and J. Daligault, Phys. Plasmas **21**, 055707 (2014).
[48] N. R. Shaffer, S. D. Baalrud, and J. Daligault, Phys. Rev. E **95**, 013206 (2017).
[49] A. Decoster, in *Modeling of Collisions*, edited by P. A. Raviart, Series in Applied Mathematics (Gauthier-Villars and North-Holland, Paris, 1998).
[50] J. Daligault, Phys. Rev. Lett. **96**, 065003 (2006).
[51] J. Clérouin, P. Arnault, C. Ticknor, J. D. Kress, and L. A. Collins, Phys. Rev. Lett. **116**, 115003 (2016).
[52] J. Clérouin, G. Robert, P. Arnault, J. D. Kress, and L. A. Collins, Phys. Rev. E **87**, 061101 (2013).
[53] P. Arnault, J. Clérouin, G. Robert, C. Ticknor, J. D. Kress, and L. A. Collins, Phys. Rev. E **88**, 063106 (2013).
[54] N. Desbiens, P. Arnault, and J. Clérouin, Phys. Plasmas **23**, 092120 (2016).
[55] T. Ott, M. Bonitz, L. G. Stanton, and M. S. Murillo, Phys. Plasmas **21**, 113704 (2014).
[56] H. D. Whitley, W. E. Alley, W. H. Cabot, J. I. Castor, J. Nilsen, and H. E. DeWitt, Contrib. Plasma Phys. **55**, 413 (2015).